Formate Over-Oxidation Limits Industrialization of Glycerol Oxidation Paired with Carbon Dioxide Reduction to Formate

DOI:
10.1002/cplu.202300112

Document status and date:
Published: 01/04/2023

Document Version:
Publisher's PDF, also known as Version of Record (includes final page, issue and volume numbers)

Please check the document version of this publication:

• A submitted manuscript is the version of the article upon submission and before peer-review. There can be important differences between the submitted version and the official published version of record. People interested in the research are advised to contact the author for the final version of the publication, or visit the DOI to the publisher's website.
• The final author version and the galley proof are versions of the publication after peer review.
• The final published version features the final layout of the paper including the volume, issue and page numbers.

Link to publication

Download date: 04. Oct. 2023

Formate Over-Oxidation Limits Industrialization of Glycerol Oxidation Paired with Carbon Dioxide Reduction to Formate

Bart van den Bosch,*[a] Brian Rawls,[a] Maria B. Brands,[b] Christel Koopman,[a] Matthew F. Phillips,[a] Marta C. Figueiredo,[c] and Gert-Jan M. Gruter*[a, b]

Electrocatalytic CO_2 reduction processes are generally coupled with the oxidation of water. Process economics can greatly improve by replacing the water oxidation with a more valuable oxidation reaction, a process called paired electrolysis. Here we report the feasibility of pairing CO_2 reduction with the oxidation of glycerol on Ni_3S_2/NF anodes to produce formate at both anode and cathode. Initially we optimized the oxidation of glycerol to maximize the Faraday efficiency to formate by using design of experiments. In flow cell electrolysis, excellent selectivity (up to 90% Faraday efficiency) was achieved at high current density (150 mA/cm^2 of geometric surface area). Then we successfully paired the reduction of CO_2 with the oxidation of glycerol. A prerequisite for industrial application is to obtain reaction mixtures with a high concentration of formate to enable efficient downstream separation. We show that the anodic process is limited in formate concentration, as Faraday efficiency to formate greatly decreases when operating at 2.5 M formate (~10 w%) in the reaction mixture due to over-oxidation of formate. We identify this as a major bottleneck for the industrial feasibility of this paired electrolysis process.

Introduction

Electrochemical reduction of CO_2 is an attractive method to produce CO_2-based chemicals. Formate is an attractive target compound because of the high catalytic efficiencies and the high atom efficiency. Although formate is readily available and cheap, the production of formate from bio-based feedstocks such as bio-based glycerol must replace the current production method from fossil-based resources.[1] Formate can be easily converted to formic acid (acidification) or oxalic acid (thermal conversion).[2]

To improve process economics of electrochemical CO_2 reduction a valuable oxidation reaction can be performed at the anode, rather than the production of relatively non-valuable oxygen by water oxidation.[3] When the CO_2 reduction to formate is paired with an anodic process to produce formate, the production capacity per electrochemical cell area is increased and the Capital Expenditures (CAPEX) decrease. Since the costs of electrochemical cells is of great significance on the formate production costs,[4] paired electrolysis to produce formate at both electrodes can strongly reduce the formate production costs. Paired electrolysis for simultaneous production of formate at both anode and cathode is reported by CO_2 reduction coupled with oxidation of glycerol[5,6] or formaldehyde.[7] In this paper we optimize reaction conditions for the oxidation of glycerol to formate in flow cell electrolysis to pair this reaction with the reduction of CO_2 (Figure 1).

Glycerol is one of the main by-products from biodiesel production. With the increasing demand for renewable fuels from biomass, the glycerol availability increased significantly.[8,9] This bio-glycerol can be a sustainable, bio-based feedstock for commodity chemicals. Contaminants in glycerol from biodiesel production, such as water and alkali ions, can be detrimental for catalyst stability in many catalytic systems.[10] In electrocatalytic systems water and alkali ions are often added as conducting electrolyte. Electrocatalysis thus seems like an attractive method for valorization of glycerol from biodiesel production and there are various reports on electrochemical

[a] Dr. B. van den Bosch, B. Rawls, C. Koopman, M. F. Phillips, Prof. G.-
    J. M. Gruter
    Renewable Chemistries
    Avantium Chemicals
    Science Park 408, 1098 XH Amsterdam (The Netherlands)
    E-mail: Bart.vandenbosch@avantium.com
    Homepage: http://www.avantium.com/technologies/volta/
[b] M. B. Brands, Prof. G.-J. M. Gruter
    Van 't Hoff Institute for Molecular Sciences
    University of Amsterdam
    Science Park 904, 1098 XH Amsterdam (The Netherlands)
    E-mail: G.J.M.Gruter@uva.nl
[c] Prof. M. C. Figueiredo
    Chemical Engineering and Chemistry
    Technical University Eindhoven
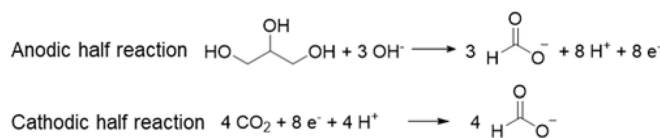   Het Kranenveld 14, 5600 MB Eindhoven (The Netherlands)

Figure 1. Equations of the two half reactions of the paired electrolysis process to produce formate at both electrodes.

glycerol oxidation to produce formate.[11–14] The atom efficiency of glycerol electro-oxidation to produce formate is excellent; the increase in molecular weight from glycerol to three formate ions is 46%, where the added weight comes from water as cheap feedstock. The process of paired glycerol oxidation and CO_2 reduction has a potential 75% increased formate production capacity per cell area compared to an 'unpaired' CO_2 reduction process, assuming full efficiency for cathodic and anodic reactions. A prerequisite for industrial feasibility of such paired electrolysis process is to achieve product streams with significant concentrations of formate to enable feasible downstream separation of formate.[15] However, none of the reports on nickel-catalyzed glycerol oxidation for formate production address this issue. For the reduction of CO_2 to formate, concentrations up to 3.4 M (15 wt.%) are reported.[16] Operating the anodic process at high formate concentrations is one of the key objectives of this study.

Nickel-based anodes have a remarkably high selectivity in the oxidation of vicinal diols (such as glycerol) for carbon–carbon bond cleavage, yielding the corresponding carboxylates.[17–19] In this work we use nickel foam (NF) coated with nickel sulphide (Ni_3S_2) nanostructures. The Ni_3S_2 nanostructures form a high electroactive surface area on the nickel foam, which results in a large increase in catalytic activity compared to plain nickel foam.[20,21] An advantage of Ni_3S_2 nanostructures over nickel oxide–hydroxide (NiOOH) nanostructures is that Ni_3S_2 is a conductor, while NiOOH is a semiconducting material.[22] Initially we study the electrosynthesis of formate from glycerol on Ni_3S_2/NF anodes at low formate concentrations. Goal is to optimize Faraday efficiency (FE) to formate at a minimum current density of 100 mA/cm². Stability studies are out of scope of this report. Excellent selectivity is achieved (up to 90% FE) at high rates (up to 150 mA/cm² of geometric electrode area). We demonstrate the paired process of glycerol oxidation and CO_2 reduction at 100 mA/cm² with good FE's (around 80% at both electrodes). When performing the oxidation of glycerol to formate with increased formate concentration in the reaction mixture (2.5 M, ∼10 wt.%), the selectivity to formate drops dramatically and a decrease in formate concentration occurs due to over-oxidation of formate. We believe that this is a major bottleneck for industrial application and this issue must be addressed with high priority to enable industrial application of paired glycerol and CO_2 electrolysis.

Results and Discussion

Ni_3S_2/NF anodes of 2 cm² are synthesized by thermal decomposition of an organic sulfur source in water in the presence of nickel foam, according to a previously reported procedure.[20] Since the maximum volume capacity of the reactor was reached, for the production of 10 cm² electrodes we could not linearly scale the reaction volume with the total electrode area. Larger electrodes for flow cell experiments are synthesized by simply elongating the reaction time. Since this hydrothermal synthesis method makes the electrodes more brittle, optimized

reaction times were found to produce electrodes with good mechanical durability and sufficient electro-active area. However, because of this brittleness, for electrodes much larger than 10 cm² we advise alternative synthesis methods, such as electrodeposition. X-ray diffraction (XRD) studies were performed on plain nickel foam and on a freshly synthesized Ni_3S_2/NF electrode (SI 1). After the hydrothermal synthesis of Ni_3S_2, four small signals (at 31, 38, 50 and 55 2-theta angles) corresponding to Ni_3S_2 appear in the diffractogram.[23,24] More intense signals corresponding to Ni_3S_2 are obtained by performing XRD on the powder of a finely crushed electrode obtained by grinding the anode with mortar and pestle (SI 1). The formation of Ni_3S_2 on the nickel surface is validated. XRD is also measured on Ni_3S_2/Ni anode after performing >10 h of electrolysis with this anode. Here we see no significant changes in the diffractogram (SI 1). Other possible crystalline phases of nickel oxides, sulfides and chlorides were not observed in the diffractograms. Scanning electron microscopy shows that the macro-structure of the nickel foam remains intact. At higher magnifications we see a homogeneous distribution of Ni_3S_2 nanorods over the surface (Figure 2 a–b).

The catalytic activity of the Ni_3S_2/NF anode towards glycerol oxidation (SI 2) was assessed with cyclic voltammetry (CV) and linear sweep voltammetry (LSV). The CV of the Ni_3S_2/NF in 1 M KOH reveals the reversible Ni^{II}/Ni^{III} oxidation.[23] In the Ni^{III} state, the electrode turns from grey/black to an intense black color,, possibly by formation of NiOOH on the surface.[20,23] In the LSV in the presence of glycerol we observe increased oxidative currents, just before the onset potential of the Ni^{II}/Ni^{III} oxidation (SI 2 and figure 4). These observations are indicative of electrocatalytic glycerol oxidation, according to the following mechanism:[17]

$$n\ Ni^{3+} + \text{glycerol} + x\ OH^- \rightarrow n\ Ni^{2+} + \text{product} + n\ H^+$$
$$n\ Ni^{2+} \rightarrow n\ Ni^{3+} + n\ e^-$$
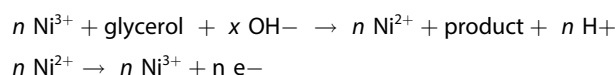
The slight cathodic shift of the catalytic onset potential compared to the onset potential of the Ni^{II}/Ni^{III} couple could be explained by an adsorption of glycerol on the catalyst surface.
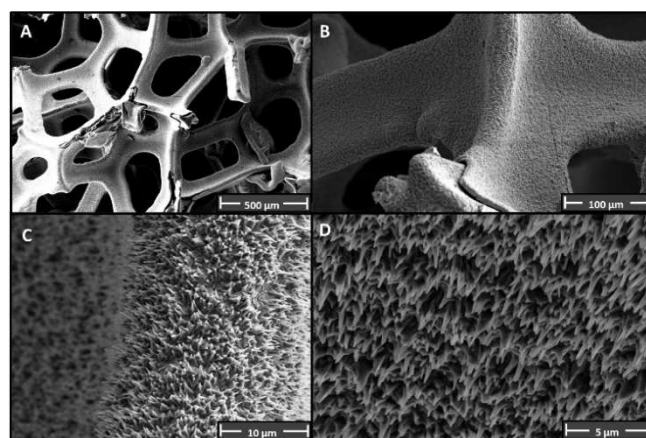

Figure 2. SEM images of the Ni_3S_2/Ni catalyst (Magnifications: A=100x, B=500x, C=3500x, D=15000x).

ChemPlusChem

Research Article
doi.org/10.1002/cplu.202300112

Chemistry
Europe
European Chemical
Societies Publishing

The number of electrons (n) and hydroxide ions (x) involved in the reaction depends on the product that is formed ($n = 8$, $x = 3$ for formation of 3 formate, $n = 6$, $x = 2$ for glycolate + formate and $n = 10$, $x = 3$ for formate + oxalate).

Identification of the products of glycerol oxidation on Ni_3S_2/NF was performed by electrolysis in a glass H-cell and monitoring the concentrations of organics with high-performance liquid chromatography (HPLC) and ion exchange chromatography (IC). The compounds determined with these methods are glycerol, formate, oxalate, glycolate and glyoxylate. During all electrolysis experiments we operate under controlled current density and measure the cell potential. The duration of the electrolysis experiment is expressed in Faraday of charge passed (Q) per molecule of substrate. This charge (Q) is expressed in FC/mol of substrate, where F = Faraday's constant (96485) and C is charge in Coulombs. A theoretical full conversion of glycerol to 3 formate ions corresponds to the passing of 8 electrons per molecule of substrate, or 8 FC/mol. For reference, an H-cell experiment with 50 mM initial glycerol concentration could convert all glycerol to formate at 100 mA/cm^2 at a minimum of 2 h and 40 min. Supporting Information 3 depicts the concentration profile and cell potential during an electrolysis experiment where a constant current of 100 mA/cm^2 is applied. Glycerol is fully converted after 8 F/mol. The main product is formate. Traces of oxalate and glycolate are observed in the reaction mixture. Initial FE's (at 2 FC/mol) are 53 % (200 mA/cm^2), 80 % (100 mA/cm^2) and 90 % (150 mA/cm^2) (Figure 3, see Supporting Information 4 for the calculation of the FE). When glycerol is depleted (after 6 FC/mol), a reduction in formate concentration is observed and the FE decreases (Figure 3 and Supporting Information 3).
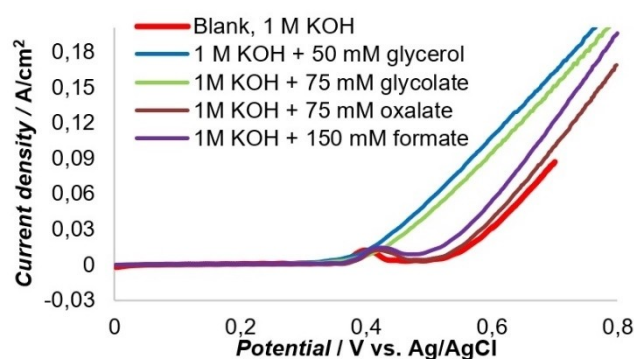
Here formate is converted into products which were not included in our analytical methods. This is reflected in a decrease in the carbon mass balance over time (the carbon mass balance is the percentage of carbon recovered in the product mixture with respect to the initial total amount of carbon). After passing of charge of 6 FC/mol at 100 mA/cm^2, 92 % of the carbon atoms were accounted for in the identified products. After a charge of 8 FC/mol this was only 73 % (Figure 5). Carbons are likely lost from the carbon mass balance
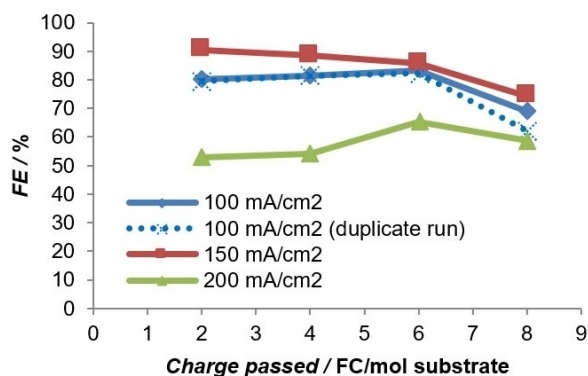
by oxidation of formate to CO_2, which can form $KHCO_3$ in the alkaline electrolyte.[17] This formate oxidation is reported to occur at higher potential than glycerol oxidation,[17] and the oxidation of formate after glycerol depletion is accompanied with an increased cell potential (SI 3). We also observe this with linear sweep voltammetry experiments where the activity of Ni_3S_2/NF anodes for glycerol and formate oxidation is compared. In the presence of 0.1 M glycerol a steep catalytic current is observed in the LSV. In the presence of 0.1 M formate, a much smaller catalytic current at a later onset potential is observed (Figure 4), reflecting the lower reactivity of formate compared to glycerol. In a competition experiment, preferential oxidation of glycerol over oxidation of formate is observed. In this competition experiment, electrolysis is started with 0.046 M formate and 0.006 M glycerol. Glycerol was fully converted first, after which the cell potential increased and formate was oxidized (see Supporting Information 5 for concentration profile and cell potential). This preferential oxidation of glycerol is discussed later in this report as a strategy to abate formate oxidation by having a high glycerol concentration in the reaction mixture.

The oxidation of oxalate and glycolate was studied since traces of these compounds are observed during glycerol oxidation. The carbons in oxalate have a higher oxidation state than carbon in formate (C^{3+} in oxalate and C^{2+} in formate). Oxalate is thus not an intermediate to formate, as this would imply a reductive reaction. In an electrolysis experiment, where oxalate is the only organic substrate, we see that oxalate is relatively unreactive under catalytic conditions (see Supporting Information 6 for the concentration profile during electrolysis), with a carbon mass balance of 95 % after passing of 12 F/mol (Figure 5). The reaction conditions were similar as for the glycerol electrolysis experiments. The relative stability of oxalate is supported with LSV with 75 mM oxalate, where only a minor increase in current compared to the blank is seen (Figure 4). Glycolate is completely oxidized under the same catalytic conditions. After passing of charge of 5 to 6 FC/mol, glycolate conversion is complete to yield formate and oxalate. (see Supporting Information 7 for the concentration profile during electrolysis). A low FE to formate is achieved (20 % after theoretical full conversion (2 FC/mol)). This low FE is likely the

Figure 3. FE towards formate on Ni_3S_2/NF anodes with current densities of 100, 150 and 200 mA/cm2. The passing of 2 FC/mol corresponds to 40 min, 26 min and 20 min for 100, 150 and 200 mA/cm^2 respectively.

Figure 4. LSV of Ni_3S_2 in the absence and in the presence of organic compounds. Scan speed = 5 mV/s.

ChemPlusChem

Research Article
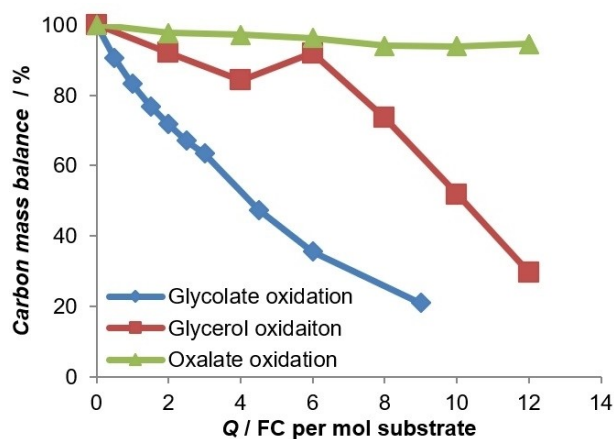doi.org/10.1002/cplu.202300112

Chemistry Europe
European Chemical
Societies Publishing

Figure 5. Carbon mass balance during the electrolysis of glycolate, glycerol and oxalate at 100 mA/cm^2.

Figure 6. Reactions observed during electro-oxidation of glycerol on Ni$_3$S$_2$/NF anode. C$_1$ indicates the formation of either formate or CO$_2$.

result of formate over-oxidation; already after 2 FC/mol 28% of the carbon is lost in the carbon mass balance (Figure 5).

In the LSV with 0.1 M glycolate, a high oxidative current is observed, comparable to that for catalytic glycerol oxidation (Figure 4). In an electrolysis experiment, we observe competition between glycerol oxidation and glycolate oxidation. In this experiment, 0.050 M glycolate is oxidized in 1 M KOH with 100 mA/cm^2, resulting in a steady decrease of glycolate (1.3×10^2 mmol/min). After 20 min glycerol (0.050 M) is added, and the conversion rate of glycolate is decreased to 0.4×10^{-2} mmol/min. The glycerol conversion rate is faster (0.7×10^{-2} mmol/min) and glycerol is depleted before glycolate is depleted (see Supporting Information 8 for the concentration profile during electrolysis). This shows that glycolate and glycerol oxidation occur but are competing pathways. Glycerol is oxidized faster than glycolate when both are present in the mixture.

Summarizing, in the electrolysis experiments performed in a glass H-cell we demonstrated that high FE (up to 90% at 150 mA/cm^2) is obtained in the oxidation of glycerol to formate. Formate is prone to over-oxidation. When glycerol and formate are present, glycerol is preferentially oxidized. Traces of oxalate and glycolate are produced in the oxidation of glycerol. Glycolate can be further oxidized to formate, CO$_2$ and oxalate, but low FE due to formate oxidation is obtained in the absence of glycerol. Oxalate is stable under catalytic conditions. Figure 6 depicts the possible products from glycerol oxidation.

These results show the following trend in relative oxidation rates for these substrates: glycerol > glycolate > formate > oxalate. It is previously suggested that the vicinal diol structure is required for highly selective C–C bound cleavage on nickel anodes.[17] Glycolate, formate and oxalate lack such a vicinal diol structure and show lower selectivity to formate and lower oxidation rates than glycerol.

To better mimic industrial conditions we explored the optimal conditions for upscaling this reaction to parallel plate flow cells. One variable is the initial concentration of glycerol (0.05, 0.525 and 1 M). To study the reaction at higher glycerol
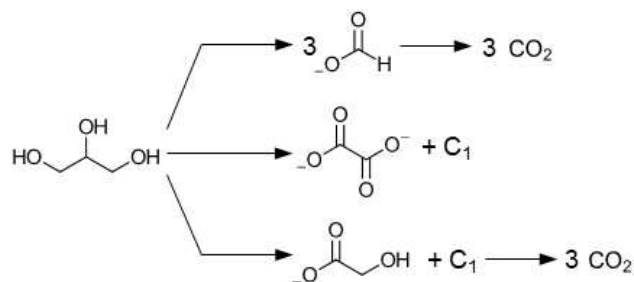
concentrations it is crucial to control the pH during the experiment; every formed molecule of formic acid neutralizes one molecule of KOH. In the experiments performed in the H-cell we avoided the need of pH control by limiting the study to low substrate concentrations. In the following flow cell experiments 17 M KOH is added with a pump during the experiment to maintain a stable pH. Extreme caution and safety precautions must be taken when working with such corrosive liquids. Another variable in flow cell electrolysis is the rate at which glycerol is fed to the anode (molar glycerol feed). This rate is dependent on the flow speed and the substrate concentration. The ratio between the molar glycerol feed at the electrode and the maximum rate of substrate conversion is referred to as the excess substrate feed, and is expressed by the Equation (1). The maximum rate of glycerol conversion is controlled by the total current.

$$Excess\ substrate\ feed = \frac{[\text{glycerol}]^* V}{\frac{i}{nF}} \tag{1}$$

where: [glycerol] is the initial glycerol concentration (M), V is the flow rate (mL s^{-1}), I is the current (A), n = number of electrons, and F = Faraday's constant.

We constructed a Design of Experiments (DoE) using JMP software to study the influence of the following factors on the FE to formate: the initial glycerol concentration (tested at 0.05, 0.525 and 1 M) and the excess substrate feed (tested at 5, 62.5 and 120). As the glycerol depletes during the experiment, the excess substrate feed will decrease. For the values in the DoE, the excess substrate feed is defined at initial glycerol concentration. The FE is determined at 33%, 66% and 99% of theoretical full conversion (corresponding to 2.7, 5.3 and 8 FC/mol). The flow experiments were performed in batch mode, recirculating the electrolytes through the electrochemical cell. The flow rate of each experiment was set by solving Equation (1) at the initial substrate concentration. The set of experiments and results are given in Table 1. We see a large spread in the FE to formate from 14% to 81% by varying the glycerol concentration and the excess substrate feed. The FE of 81% was achieved at 0.05 M glycerol and an excess substrate feed of 120.

The three main effects of the aforementioned factors, with their six interactions and their 2nd order effects were considered

ChemPlusChem

Research Article
doi.org/10.1002/cplu.202300112

**Chemistry
Europe**
European Chemical
Societies Publishing

Table 1. DoE performed for optimizing FE to formate (= response) with the glycerol concentration and excess feed as factors.

Experiment #	[Glycerol]/ M	Excess substrate feed	Theoretical conversion/%	FE/%
1	0.05	5	33	69
	0.05	5	99	64
2	0.05	120	66	81
3	1	120	33	55
	1	120	99	50
4	1	62.5	66	56
5	0.05	120	33	74
	0.05	120	99	71
6	0.05	62.5	66	72
7	1	5	33	46
	1	5	99	14
8	1	120	66	58
9	0.525	62.5	99	61
10	0.525	5	66	54

for selecting a model. An interaction between factors is significant when the effect of one factor on the FE is dependent on the value of the second factor. A second order effect is relevant when there is curvature in the FE with respect to that factor. The Bayesian information criterion (BIC) was used to select a model that fits this data while avoiding overfitting of the model.[25] Glycerol concentration, excess substrate feed, their interaction, and the second order effect of excess substrate feed were selected for the final model resulting in an R^2 value of 0.904. This signifies that the model explains 90.4% of the variation in the response. The coefficient of each effect in the model and the confidence interval ($\alpha=0.05$) are shown in Supporting Information 9. The script for obtaining the model in JMP 16 is given in Supporting Information 10.
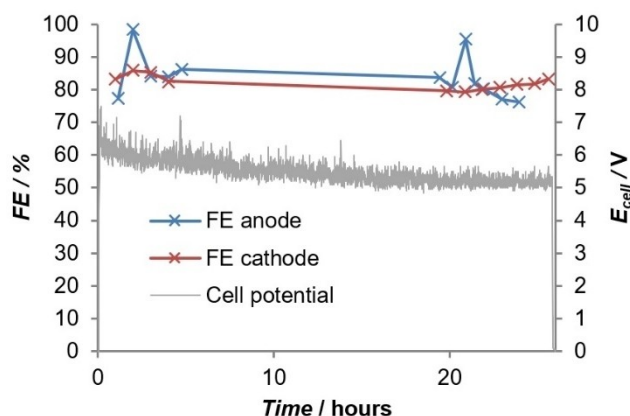
An effect has a larger influence on the response if the absolute value of its coefficient is larger. Furthermore, the effect is statistically significant when its coefficient confidence interval does not overlap with zero (i.e. the coefficient is nonzero). Therefore, the initial glycerol concentration appears to be the most influential factor (coefficient estimate = −33.55) as well as statistically significant while the excess feed rate is seen to be the second most influential factor (coefficient estimate = 0.12) and statistically significant. The interaction effect and the second order effect of excess feed are the third and fourth most influential effects respectively. However, these two effects could potentially have a true coefficient value of zero. Further experimentation would be necessary to confirm or deny their true significance. The model resulting from the DoE is graphically presented in Figure 7. The equation for the model is given in Supporting Information 11. The FE is significantly affected by both the excess substrate feed and the initial glycerol concentration. The negative coefficient for the [glycerol] term in the model indicates a decreased FE with increasing glycerol concentration. Conversely, the positive coefficient of the excess feed term indicates a higher FE to formate with increasing excess feed, showing a maximum around ESF = 70. For maximizing the FE to formate we should operate at low substrate concentration and excess substrate feed around 70.
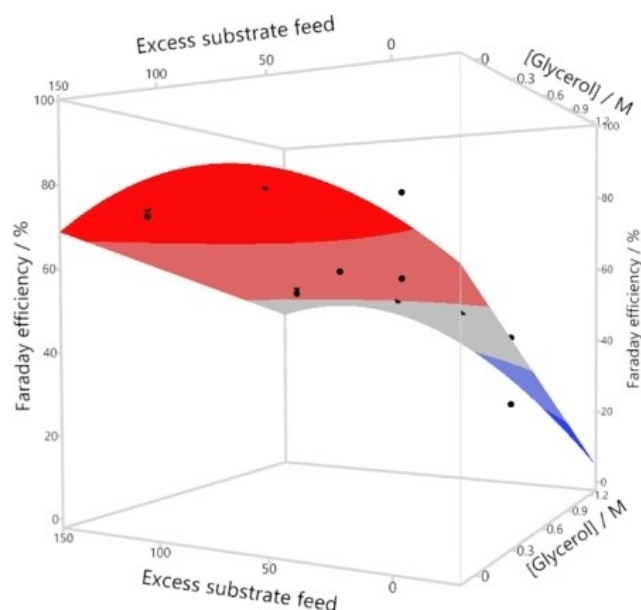
Figure 7. A graphical presentation of the model obtained from the DoE. The red-blue contour plot depicts the formulae obtained from the model equation (SI 11). The black dots indicate actual data points.

Pairing glycerol oxidation and CO₂ reduction

With these optimized conditions ([glycerol] = 50 mM, ESF = 70), the oxidation of glycerol was paired with CO_2 reduction to formate. The cathodic process was performed with a Gas-Diffusion Electrode (GDE) containing indium–bismuth nanoparticles (InBi NP's). The GDE and InBi NP's are synthesized according to literature procedure.[26] The electrochemical cell consists of three compartments (anolyte, catholyte and CO_2 gas compartment at the back of the GDE). The anodic and cathodic compartment are separated by a bipolar membrane (BPM). The use of a BPM was required to maintain a stable pH at both compartments; a cation exchange membrane would result in potassium transport from anode to cathode, causing a drop in anodic pH over time. An anion-exchange membrane would result in unwanted formate and/or carbonate transport from cathode to anode. Figure 8 depicts the FE for both the anodic

ChemPlusChem

Research Article
doi.org/10.1002/cplu.202300112

**Chemistry
Europe**
European Chemical
Societies Publishing

Figure 8. FE of the anodic and cathodic process in the paired electrolysis of glycerol oxidation and CO_2 reduction and the cell potential over a period of 24 h at 100 mA/cm^2.

and cathodic reactions and the cell potential during 24 h electrolysis at 100 mA/cm^2.

Good FE's are obtained for anodic (between 77–98%) and cathodic (79–83%) reactions, with a cell potential between 5 and 6.3. No decrease in cathodic efficiency is observed. The anodic process seems to lose some efficiency towards the end of the experiment. From this experiment it cannot be concluded if this is actual system degradation or an artefact. The paired electrolysis of glycerol and CO_2 for the production of formate is previously reported, [6] but to the best of our knowledge, the current density of 100 mA/cm^2 is unprecedented in this paired process.

Formate concentration in the anodic process

Our next priority was to study the feasibility of operating the anodic process at relevant formate concentrations. An envisioned continuous process would operate in steady state at formate concentrations sufficiently high for downstream processing. We know that formate is prone to oxidize, especially when there is no glycerol present in the reaction mixture. Initially we performed LSV with increasing amounts of formate to show the dependence of formate oxidation rates on the formate concentration. We see significant catalytic current corresponding to formate oxidation, especially at increased formate concentrations (Supporting Information 12). However, glycerol oxidation at a concentration of 50 mM glycerol still occurs at lower onset potential and results in higher current density, even compared to the current density for formate oxidation at 2.15 M formate. With electrolysis experiments we study the effect of formate and glycerol concentrations on the production rate of formate. We defined a formate concentration of 2.5 M (~ 10 wt.%) as the minimum concentration for feasible downstream separation, although clearly even higher concentrations are preferred. In the next electrolysis experiments we start with 2.5 M formate in the mixture. Electrolysis experiments are ran in batch, by recirculating the electrolyte through the

electrochemical cell. Since we know from previous results that the glycerol concentration can affect the rate of formate oxidation, we performed electrolysis at three different initial glycerol concentrations (0.05, 0.55 and 1.1 M). The reaction mixtures are analysed for carbonate after electrolysis, as CO_2 from formate oxidation can form carbonates in the alkaline electrolyte. The concentrations of all compounds are corrected for changes in electrolyte volume during the experiments. Figure 9 depicts the formate production over time, and thus the slope of the lines is the formate production rate in mmoles/minute. For comparison the formate production rate for a theoretical 100% FE to formate is depicted (red line). This line is determined by the applied current (9.25 A) and is calculated according to following equation:

$$formate\ production\ rate = \frac{i}{nF}*t*FE$$

where: $i =$ current (A), $n =$ number of electrons ($= 8$), $F =$ Faraday's number, $t =$ time (seconds).

Remarkably, for each electrolysis run a negative formate production rate is observed, indicating that over-oxidation of formate occurs at a faster rate than formate production. This is supported by the formation of (bi)carbonate in the reaction mixture after electrolysis (total formation of bicarbonate after electrolysis is 5; 6 and 10.5 mmoles @ 0.05; 0.55 and 1.1 M initial glycerol concentration respectively). No formate was observed in the catholyte solutions after electrolysis, and the possibility of formate transfer through the membrane is excluded.

The least negative formate production rate is observed at 1.1 M initial glycerol concentration. We speculate that the high glycerol concentration abates formate over-oxidation to a certain extent by preferential glycerol oxidation. However, at 0.05 M initial glycerol concentration the formate production rate is less negative than at 0.55 M initial glycerol concentration. This could be the result of lower selectivity to formate at 0.55 M glycerol than at 0.05 M, as is also reflected in Figure 7 in the model obtained from the DoE. This is supported by the fact that at 0.55 M and 1.1 M initial glycerol concentration, significant FE's to glycolate (24% and 17% for 0.55 M and 1.1 M initial
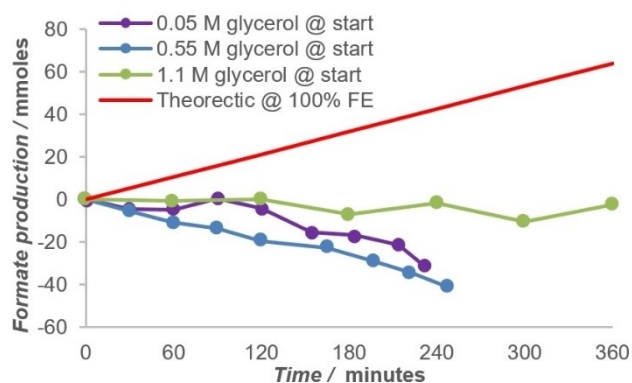
Figure 9. Formate production rate for electrolysis experiments with 2.5 M formate at the start and the theoretic formate production when 100% FE is assumed (red line).

glycerol concentration respectively) and glyoxylate (1% and 7% for 0.55 M and 1.1 M initial glycerol concentration respectively) are observed.

In summary, when operating the anodic process at 2.5 M formate, the selectivity to formate drops dramatically, and even a decrease in formate concentration is seen, due to over-oxidation of formate. This means that the anodic catalyst system described here is not suited for industrial purposes, as no relevant formate concentrations can be achieved.

Conclusions

We demonstrate that Ni_3S_2 anodes have great catalytic properties for glycerol oxidation to formate at low concentrations of formate, with high selectivity at high current density. This anodic process was successfully paired with CO_2 reduction to produce formate at both electrodes. Such a paired electrolysis process has great potential to reduce the production costs of formate by electrochemical CO_2 reduction, since the production capacity per electrode area is significantly increased. We show that the industrial application of this process for this specific catalyst system is hampered by the inability to operate the anodic process at high formate concentrations; at 2.5 M formate a decrease in formate concentration is observed during electrolysis due to formate over-oxidation. This is a critical issue to solve, as downstream separation of formate from the aqueous reaction mixture requires significant concentrations (>10 wt.%) of formate. A possible strategy to improve the efficiency to formate at high formate concentrations is to operate at a controlled potential. Since formate oxidation is more sluggish than glycerol oxidation at lower potentials, an increase in FE to formate can be expected when operating under controlled potential rather than under controlled current density. However, for the catalyst described here this would not result in sufficient current density, as we set the lower limit for current density at 100 mA/cm². Accepting lower current densities can result in higher FE to formate for this catalyst. Alternative catalysts can be developed that have even higher activity glycerol oxidation in the potential window where formate is stable. This can for instance be achieved by alternative catalyst metals, doping of the catalyst and/or increasing the electro-active area.

Experimental Section

Materials and Methods: Nickel foam (pore size 800 μm, 460 g/m², 2.5 mm thick) was purchased at Alantum. Thiourea (ACS reagent, >99.0%), glycerol (≥99.5%) and glycolic acid (ReagentPlus, 99%) were purchased from Sigma Aldrich. Potassium glycolate was made in situ by adding equimolar amounts glycolic acid and KOH. Potassium oxalate hydrate (99%) and potassium formate (99%, water <2%) were purchased from Alfa Aesar. Current densities (J) are reported as current per geometric electrode surface area (mA/cm²).

Methods for product analysis and electrode analysis: High Performance Liquid Chromatography (HPLC) was used to determine glycerol, formic acid, oxalic acid and glycolic acid concentration. HPLC was performed on an Agilent 1260 Infinity II system with 1260 series refractive index (RID) and diode array (DAD WR) detectors. The column was an Aminex HPX-87H (300×7.8 mm; dp 9 μm). 7 μL sample was injected and separated using 5 mM H2SO4 in MilliQ water (flow rate: 0.6 mL.min, 30 °C) as the mobile phase.Ion exchange chromatography (IC) was used to (bi) carbonate concentrations. IC was performed with a Thermo Scientific Dionex ICS 5000 equiped with a Dionex DRS 600 4 mm ion suppressor and conductivity detector. The column was an Ion Pack AS19 Dionex (4×250 mm). 3 μL sample was injected and separated using a gradient. The mobile phase (flow rate: 1 mL/min, 30 °C) consisted of a mixture of MilliQ water (solvent A) and 0.5 M sodium hydroxide in MilliQ water (solvent B). The initial percentage of solvent B was 2% at 0 min and increased linearly from 2% at 2 min to 4% at 7 min and maintained at 4% during 7–14 min. At 14.1 min, the eluent was restored to the initial conditions. X-ray diffraction was performed on a MiniFlexII diffractometer (Japan, Rigaku), which uses Ni-filtered $CuK\alpha$ radiation from an X-ray tube operated at 30 kV and 15 mA. The sample is prepared by mounting the electrode on a glass plate. The Ni_3S_2/NF sample is rotated at a rate of 1.5 deg/min and the Ni foam sample is rotated at a rate of 2.5 deg/min, from an angle of 10° to 90°.

Hydrothermal synthesis of Ni_3S_2/NF anodes: Nickel foam (1 cm× 2 cm or 3.7 cm×2.5 cm) was sonicated: first in acetone (5 min), next in 3 M HCl (5 min), and finally in water (2 times 10 min). The nickel foam piece was then rinsed with water and acetone and then left to dry for at least 2 h. 36 mL of 0.23 M thiourea in water was poured into a 45 mL PTFE cup placed in a Parr Acid Digestion Vessel (no. 4744). After immersing the nickel foam in this solution it was shaken to ensure a homogeneous mixture and proper submersion of the electrode. The reactor was then placed in an oven at 180 °C. The reaction times were four hours for 2 cm² electrodes and 17 h for 11 cm² electrodes. After cooling down to room temperature the Ni_3S_2/Ni piece was rinsed with water and left to dry. The color of the piece changed from grey (nickel foam) to a darker grey (Ni_3S_2/NF).

Cyclic voltammetry and linear sweep voltammetry: Cyclic Voltammetry (CV) and Linear Sweep Voltammetry (LSV) studies were carried out in a three-electrode undivided cell with a potentiostat/galvanostat (PGSTAT 100N, Metrohm-Autolab). Platinum (Pt) gauze was used as counter electrode, a leak free Ag/AgCl electrode in 3.4 M KCl solution as reference electrode and 1 cm² Ni_3S_2/NF as working electrode. The rest of the electrode was covered with epoxy. 1 M KOH was used as electrolyte and when required substrate was added to obtain 0.05 M of substrate. The reactions were carried out at room temperature and were stirred at 1000 rpm.

Bulk electrolysis in H-cell: Bulk electrolysis experiments were performed in an H-cell with glass frit separator with 25 mL of 1 M KOH as supporting electrolyte in both compartments and substrate only at the anode side. Ni_3S_2/Ni (1 cm² geometric surface area) was used as anode. Platinum gauze was used as cathode. Glycerol electrolysis: Glycerol (91.4 μL; 115.1 mg; 1.25 mmol; 0.05 M) was added to the anolyte. The current was set at 100 mA, 150 mA or 200 mA. The total experiment time was 2 h 40 min, 1 h 52 min and 1 h 20 min respectively. The total amount of charge that passed through the cell corresponded to 8 F Coulomb per mole of glycerol (where F = Faraday's constant (96485)). Samples for IC analysis were taken from the anolyte every 40 min and a sample of the catholyte was taken after electrolysis. Glycolate and oxalate electrolysis: Experimental conditions are similar to those for glycerol oxidation, starting with potassium glycolate (142 mg, 0.05 M) or potassium oxalate (145 mg, 0.05 M). The current density was 100 mA/cm². Competition experiment potassium formate and glycerol oxidation:

ChemPlusChem

Research Article
doi.org/10.1002/cplu.202300112

Chemistry
Europe
European Chemical
Societies Publishing

Potassium formate (97 mg, 0.46 M) and glycerol (11 μL, 0.006 M) was added to the anolyte. A constant current (100 mA) was applied for 1 h. Samples are taken every 10 min. <u>Competition experiment potassium glycolate and glycerol oxidation:</u> Potassium glycolate (142 mg, 0.05 M) was added to the anolyte. A constant current (100 mA) is applied for a total of 6 h. After 20 min glycerol (91 μL, 0.05 M) is added.

Flow cell electrolysis: The flow cell experiments were performed in batch configuration by recirculating the electrolytes from external reservoirs through the electrochemical cell (Electrocell Micro Flow Cell). On the cathode side 0.1 M $KHCO_3$ with constant purging of CO_2 (0.15 L/min) was used as electrolyte. Platinum gauze (2.2× 5 cm) was used as cathode. On the anode side 1 M of KOH was used as supporting electrolyte with the appropriate concentration of glycerol (unless stated otherwise). Ni_3S_2/NF (2.2×5 cm) was the anode. As membrane a Fumasep FBM Bipolar Exchange Membrane with PK reinforcement was used. Prior to cell assembly this membrane was pre-treated by heating it to 50 °C for 2 h in 1 M KOH. The gap between the electrodes and the membrane was 2 mm at both anodic and cathodic compartments. The catholyte flow was set at 80 mL/min and kept constant for all the experiments. The anolyte flow was modified accordingly with the experiment and is indicated along the results. The collected samples were analysed by IC for formate, oxalate and glycolate and HPLC for glycerol.

Design of Experiments: JMP's custom design platform was used to create the DOE. The concentration of glycerol and excess substrate feed were treated as very hard and hard to change variables respectively. This resulted in a split-split-plot design to reduce the number of flow cell experiments necessary to screen the three factors while considering factor interactions and square term effects.

Production of gas diffusion layer (GDL): 8.92 mL of PTFE DISP 30 was added to 70 mL of a 1:1 volume IPA/water mixture and stirred for 1 min before mixing with 15 g of Soltex Acetylene Black 75%-03 carbon in a Bourgini mixer. After 1 min of mixing, a dough-like mixture was collected. A rolling pin was used to prepare the dough for a cross-rolling technique to obtain the desired thickness, where the thickness setting is a discrete numerical factor. A rectangle of about 250 cm^2 was cut from, and a paint roller was used to apply PTFE DISP 30 diluted to 50% with a 1:1 volume IPA/water to the back of the dough. Fiber Glas 1 K plain weave carbon fiber fabric was used as the current collector and placed on top of the PTFE-applied layer. A Carver heated press (model number 4533) was used to press the structure in three stages at various temperatures (100–360 °C, pressures (5–45 ton) with a 30 min duration per stage.

Production of In−Bi NP's coated GDE: For the synthesis of the catalyst 620 mg $InCl_3$, 680 mg $BiNO_3.5H_2O$ and 882 mg trisodium citrate are heated to 100 °C in 100 mL tri-ethylene glycol in N_2 atmosphere. 4 mL $NaBH_4$ in water is added dropwise over the course of 1 minute, after which the solution was stirred 15 min. The mixture was stirred at room temperature overnight. Acetone is added to a final volume of 300 mL. This mixture is divided over 8 centrifuge tubes and centrifuged at 8000 rpm for 25 min. After separating particles from supernatant by decantation the particles are suspended in IPA, and again centrifuged at 8000 rpm for 25 min. The decantation, suspension in IPA and decantation is repeated once. The resulting particles are suspended in 90 mL IPA and sonicated for 20 min. 0.077 g PVDF (Kynarflex) in 90 mL acetone is prepared. The resulting PVDF mixture and catalyst mixture are alternating airbrushed layer by layer on the 9.25 cm^2 GDL. The GDE is left to dry overnight and used in the paired electrolysis experiment.

Paired electrolysis: The anodic process was ran as described in the section flow cell electrolysis ([glycerol] = 50 mM, ESF = 100). The cathodic process was operated in 0.5 M $KHCO_3$, which was recirculated through the cathode compartment at 50 mL/min. The catholyte volume was 0.3 L. The pH of the catholyte is controlled between 7.1 and 7.3 by automated dosing of 3 M $KHCO_3$ in water. The CO_2 gas was fed to the gas compartment at the back of the GDE at 50 mL/min.

Conflict of Interest

The authors declare no conflict of interest.

Data Availability Statement

The data that support the findings of this study are available from the corresponding author upon reasonable request.

[1] J. Hietala, A. Vuori, P. Johnsson, I. Pollari, W. Reutermann, H. Kieczka, *Formic Acid, in Ullmann's Encyclopedia of Industrial Chemistry (Ed)* **2016**.
[2] E. Schuler, M. Morana, P. A. Ermolich, K. Lïschen, A. J. Greer, S. F. R. Taylor, C. Hardacre, G.-J. M. Gruter, *Green Chem.* **2022**, *24*, 8227–8258.
[3] J. Na, B. Seo, J. Kim, C. W. Lee, H. Lee, Y. J. Hwang, B. K. Min, D. K. Lee, H.-S. Oh, U. Lee, *Nat. Commun.* **2019**, *10*, 5193.
[4] H. Shin, K. U. Hansen, F. Jiao, *Nat Sustain* **2021**, *4*, 911–919.
[5] S. Verma, S. Lu, P. J. A. Kenis, *Nat. Energy* **2019**, *4*, 466–474.
[6] Y. Pei, Z. Pi, H. Zhong, J. Cheng, F. Jin, *J. Mater. Chem. A* **2022**, *10*, 1309–1319.
[7] M. Li, T. Wang, W. Zhao, S. Wang, Y. Zou, *Nano-Micro Lett.* **2022**, *14*, 211.
[8] C. R. Chilakamarry, A. M. M. Sakinah, A. W. Zularisam, R. Sirohi, I. A. Khilji, V. J. Reddy, A. Pandey, *Bioenerg. Res.* **2022**, *15*, 46–61.
[9] M. R. Monteiro, C. L. Kugelmeister, R. S. Pinheiro, M. O. Batalha, A. Da Silva César, *Renew. Sust. Energ. Rev.* **2018**, *88*, 109–122.
[10] S. Veluturla, N. Archna, D.Subba Roa, N. Hezil, I. S. Indraja, S. Spoorthi, *Biofuels* **2016**, *9*, 3.
[11] Y. Li, L. Chen, J. Shi, M. He, *Nat. Commun.* **2019**, *10*, 5335.
[12] X. Han, H. Sheng, C. Yu, T. W. Walker, G. W. Huber, J. Qiu, S. Jin, *ACS Catal.* **2020**, *10*, 6741–6752.
[13] M. S. E. Houache, R. Safari, U. O. Nwabara, T. Rafaïdeen, G. A. Botton, P. J. A. Kenis, S. Baranton, C. Coutanceau, E. A. Baranova, *ACS Appl. Energ. Mater.* **2020**, *3*, 8725–8738.
[14] S. Li, P. Ma, C. Gao, L. Liu, X. Wang, M. Shakouri, R. Chernikov, K. Wang, D. Liu, R. Ma, J. Wang, *Energy Environ. Sci.* **2022**, *15*, 3004–3014.
[15] B. van den Bosch, J. Krasovic, B. Rawls, A. L. Jongerius, *Curr. Opin. Green Sustain. Chem.* **2022**, *34*, 100592.
[16] L. Li, A. Ozden, S. Guo, F. Pelayo Garcia de Arquer, C. Wang, M. Zhang, J. Zhang, H. Jiang, W. Hang, H. Dong, D. Sinton, E. H. Sargent, M. Zhong, *Nat. Commun.* **2021**, *12*, 5223.
[17] S.-C. Chang, Y. Ho, M. J. Weaver, *J. Am. Chem. Soc.* **1991**, *113*, 9506–9513.
[18] Y. Li, X. Wei, L. Chen, J. Shi, M. He, *Nat. Commun.* **2019**, *10*, Article number: 5335.
[19] a) H. Ruholl, H. J. Schäfer, *Synthesis* **1988**, *1*, 54–56; b) B. V. Lyalin, V. A. Petrosyan, *Russ. J. Electrochem.* **2010**, *Vol. 46*, 1199–1214; c) M.

ChemPlusChem

Research Article
doi.org/10.1002/cplu.202300112

Chemistry Europe
European Chemical
Societies Publishing

Fleischmann, K. Korinek, D. Pletcher, *J. Electroanal. Chem.* **1971**, *31*, p 39–49.

[20] B. You, X. Liu, N. Jiang, Y. Sun, *J. Am. Chem. Soc.* **2016**, *138*, 13639–13646.

[21] L.-L. Feng, G. Yu, Y. Wu, G.-D. Li, Y. Sun, T. Asefa, W. Chen, X. Zou, *J. Am. Chem. Soc.* **2015**, *137*, 14023–14026.

[22] J. S. Chen, C. Guan, Y. Gui, D. J. Blackwood, *ACS Appl. Mater. Interfaces* **2017**, *9*, 496–504.

[23] T.-W. Lin, C.-S. Dai, K.-C. Hung, *Sci. Rep.* **2014**, *4*, 7274.

[24] N. Feng, D. Hu, P. Wang, X. Sun, X. Li, D. He, *Phys. Chem. Chem. Phys.* **2013**, *15*, 9924–9930.

[25] P. Goos, B. Jones, *Optimal Design of Experiments: A Case Study Approach*, Wiley Publishers, **2011**.

[26] M. F. Phillips, D. Pavesi, T. Wissink, M. C. Figueiredo, G.-J. M. Gruter, M. T. M. Koper, K. J. P. Schouten, *ACS Appl. Energ. Mater.* **2022**, *5*, 1720–1730.